vestigations that have been carried out in different pieces of apparatus.

Conclusions

Any of Eqs. (11), (12), or (13) together with Eq. (3) give an explicit, closed form representation of the mean velocity profile in a turbulent boundary layer which is valid over the whole width of the boundary layer and fits well the experimental data. Equations (11) and (12) are accurate explicit approximations of Spalding's formulas for the law of the wall for $\ell=3$ and $\ell=4$, respectively; while Eq. (13) is a representation of the law of the wall which better fits the experimental data.

References

[1]Coles, D. E. and Hirst, E. A., eds., "Computation of Turbulent Boundary Layers," *Proceedings of the 1968 AFOSR – IFP – Stanford University Conference,* Complied Data, Stanford University, Stanford, Calif., Vol. II, 1968.

[2]Coles, D. E., "The Law of the Wake in the Turbulent Boundary Layer," *Journal of Fluid Mechanics,* Vol. 1, July 1956, pp. 191-226.

[3]Finley, P. J., Khoo, C. P., and Chin J. P., "Velocity Measurements in a Thin Turbulent Water Layer," *La Houille Blanche,* Vol. 21, 1966, pp. 713-721.

[4]Bradshaw, P. (ed.), *Turbulence,* 2nd Ed., Springer-Verlag, Berlin, 1978, p. 136.

[5]Dean, R.B., "A Single Formula for the Complete Velocity Profile in a Turbulent Boundary Layer," *Journal of Fluids Engineering,* Vol. 98, Dec. 1976, pp. 723-726.

[6]White, F.M., *Viscous Fluid Flow,* 1st Ed., McGraw-Hill, New York, 1974, pp. 474-477.

[7]Spalding, D.B., "A Single Formula for the Law of the Wall," *Journal of Applied Mechanics, Transactions of ASME,* Series E, Vol. 83, Sept. 1961, pp. 455-458.

[8]Laufer, J., "The Structure of Turbulence in Fully-Developed Pipe Flow," NACA Report 1174, 1954 (supersedes TN 2954).

[9]Cody, W.J., Fraser, W., and Hart, J.F., "Rational Chebyshev Approximation Using Linear Equations," *Numerische Mathematik,* Vol. 12, 1968, pp. 242-251.

[10]Meinardus, G., *Approximation of Functions: Theory and Numerical Methods,* Springer-Verlag, Berlin, 1967, Chap. 9.

[11]Lindgren, E. R., "Experimental Study on Turbulent Pipe Flows of Distilled Water," Dept. of Civil Engineering, Oklahoma State Univ., Rept. 2, July 1965.

[12]Patel, V. C. and Head, M. R., "Some Observations on Skin Friction and Velocity Profiles in Fully Developed Pipe and Channel Flows," *Journal of Fluid Mechanics,* Vol. 38, Aug. 1969, pp. 181-201.

[13]Durst, F. and Rastogi, A. K., "Calculation of Turbulent Boundary Layer Flows with Drag Reducing Polymer Additives," *Physics of Fluids,* Vol. 20, Dec. 1977, pp. 1975-1985.

Turbulent Nonreacting Swirling Flows

J. I. Ramos*
Carnegie-Mellon University, Pittsburgh, Pennsylvania

Introduction

THE purpose of this work is to present some numerical results for incompressible, confined, swirling flows in a model combustor. These results have been obtained by means of the k-ϵ and k-ℓ models of turbulence[1,2] and compared with the experimental data of Vu and Gouldin.[3] The calculations have been performed in a model combustor which consists of a 3.43 cm diam inner pipe and a 14.5 cm diam outer pipe. The outside diameter of the inner pipe is 3.86 cm. The turbulence models used in this study use an isotropic eddy diffusivity whose validity in swirling flows has been seriously questioned, e.g., Ref. 4. The models solve the axisymmetric form of the conservation equations of mass; axial, radial, and tangential momentum; turbulent kinetic energy k; turbulent length scale ℓ; or dissipation rate of turbulent kinetic energy ϵ. Similar calculations have been performed by Srinivasan and Mongia,[5] who employed the k-ϵ model and who also compared their theoretical results with the experimental data of Vu and Gouldin.[3] Srinivasan and Mongia[5] concluded that the k-ϵ model had to be modified to include the effects of the curvature Richardson number in order to predict a recirculation zone for both coswirl (jets rotating in the same direction) and counterswirl (jets rotating in opposite directions) conditions. In this Note, however, it is shown that the k-ϵ model does predict a recirculation zone for both co- and counterswirl flow conditions if suitable inlet conditions are used. The effect of the inlet conditions on the flowfield has been previously investigated by Ramos,[1,2] and Abujelala and Lilley.[6] The latter showed that small changes in the inlet conditions produce drastic changes in the flowfield.

Presentation and Discussion of Results

Some representative results obtained with the k-ϵ and k-ℓ models are shown in Figs. 1 and 2. These figures present the mean axial and mean tangential velocity profiles along the combustor, i.e., at different values of z/R_i where z is the distance from the inner pipe exit and R_i is the inner pipe radius, as a function of the normalized radial distance. In these figures, the axial u and tangential w velocity profiles have been normalized by the inner jet inlet velocity which is uniform. The figures correspond to the cases A-D studied by Vu and Gouldin[3]; these cases are reproduced in Table 1. In this table, α denotes the outer-to-inner-jet inlet velocity ratio, and S_i and S_o denote the inner and outer swirl numbers.

In Figs. 1 and 2, the dots correspond to the experimental values of Vu and Gouldin.[3] However, since these investigators did not obtain fully axisymmetric flows, the data in these figures correspond to the average of the experimental values on both sides of the combustor symmetry axis. The solid and dotted lines in the figures correspond to the numerical results obtained with the k-ℓ and k-ϵ models. Figure 1 shows the mean axial velocity profiles for cases A and B,

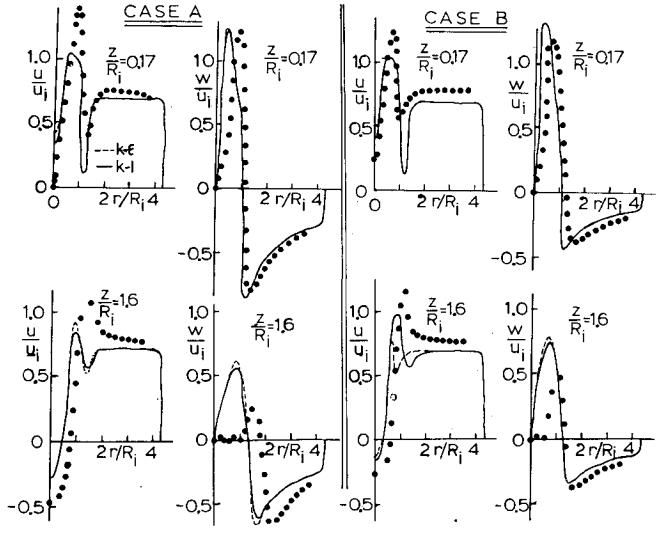

Fig. 1 Mean axial and tangential velocity profiles. Conditions A (left) and B (right).

Received Feb. 15, 1983; revision received Aug. 5, 1983.

*Assistant Professor, Department of Mechanical Engineering. Member AIAA.

i.e., for counterswirl. In case A, the inner jet is lifted by centrifugal forces. The maximum velocity appears about $r/R_i = 1.0$. There is also a minimum velocity that is due to the finite thickness of the inner pipe. The predictions tend to show a much more uniform inner jet velocity profile and do not predict the velocity minimum at the centerline and at the inner pipe.

The velocity peak has decreased at $z/R_i = 1.6$, and the minimum velocity at $r/R_i = 1$ has disappeared; however, the velocity at the centerline is now negative, i.e., a recirculation zone has been created. Neither the maximum nor the minimum velocity peaks are predicted. Figure 2 also shows the mean axial velocity profiles for conditions B (weak swirl). From this figure we see that the maximum and minimum velocities are smaller than those of condition A; in particular, the velocity minimum at the centerline is less than that of case A. However, the theory does not predict the velocity minimum at the centerline and the velocity peak at $r/R_i = 1.0$.

In Fig. 2 we show the mean axial velocity profiles for conditions C and D, i.e., zero and weak coswirl in the outer flow, respectively. Again the velocity peaks are smaller than in the two previous cases and the theory is in better agreement with the experiments; however, the velocity minimum at the centerline is not predicted at $z/R_i = 1.9$. Figure 2 also shows the mean axial velocity profiles for coswirl flow conditions. This figure is most interesting; it shows very good agreement with the experiments except at the centerline, where the theory shows a nonexisting recirculation zone. This is an important point to keep in mind: the theoretical model predicts a recirculation zone for both co- and counterswirl flow conditions, while the experiments only show a recirculation zone for counterswirl. The model is also unable to predict the velocity minimum at the centerline. Similar results were found by Habib and Whitelaw[7] for weak swirl flow conditions and by Ramos,[1,2] who used the k-ϵ model of turbulence. Habib and Whitelaw[7] claimed that this deficiency was due to the streamline curvature of the flow and the isotropic character of the turbulent viscosity. The flowfield is evidently different for co- and counterswirl. The tangential slip velocities across the interjet shear layer are progressively reduced as the flow goes from counter- to coswirl. The velocity gradients at this interjet shear layer are also reduced, as is the turbulent kinetic energy.

Figure 1 also shows the mean tangential velocity profiles for the maximum counterswirl flow conditions studied (case A). It is clear from this figure that, at $z/R_i = 0.17$, the free vortex structure of the outer jet is predicted; however, the inner flow structure is not. The magnitude of the velocity peak is predicted; however, the theoretical model shows the velocity peak closer to the centerline than the experimental data. The discrepancy seems to be due to the higher levels of

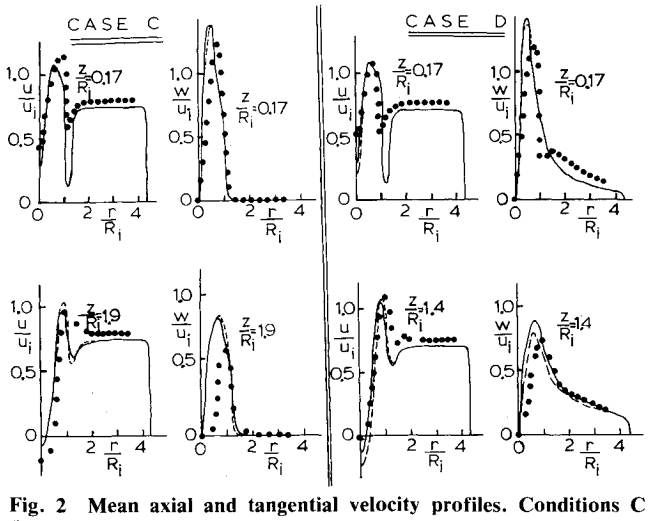

Fig. 2 Mean axial and tangential velocity profiles. Conditions C (left) and D (right).

Table 1 Inlet flow conditions for nonreacting swirling flows

Flow condition	$\alpha = u_o/u_i$	u_i, m/s	S_i	S_o
A	0.69	42.5	0.59	−0.38
B	0.68	43.2	0.63	−0.19
C	0.74	41.0	0.68	0.0
D	0.70	42.5	0.69	0.21
E	0.70	41.7	0.71	0.42

dissipation and turbulent viscosity predicted at the interjet shear layer which smooth the steep velocity gradients there. At $z/R_i = 1.6$, we observe that the outer flow structure is damped more slowly than the inner one. The agreement between theory and experiment is rather poor. The experiment also shows no inner tangential velocity. In Fig. 1 we also show the mean tangential velocity profiles for condition B. The structure of the outer flow is predicted; however, the maximum velocity is closer to the centerline than the experimentally found value. At $z/R_i = 1.6$, the inner jet velocity peak is smaller, by a factor of 2, than at $z/R_i = 0.17$; the inner jet structure is not predicted. For zero outer-swirl flow conditions (Fig. 2), the flow trends are predicted; the inner jet velocity peak is greater than that of previous figures. Figure 2 also indicates that, at $z/R_i = 1.9$, the solid body rotation does not appear in the experiment; the tangential velocity profile shows a parabolic form at the centerline. This characteristic is also shown in Fig. 1. Figure 2 also shows the mean tangential velocity profiles for weak coswirl flow conditions. The predictions are, in these two cases, in better agreement with the experimental values than for counterswirl flow conditions.

The mean axial and tangential velocity profiles for case E (cf. Table 1) are not presented here but are similar to those shown in Fig. 2 for weak coswirl conditions. In particular, both turbulence models predict a nonexisting recirculation zone under coswirl conditions. Similar results have been found by Srinivasan and Mongia,[5] who used a modified k-ϵ model. Further comparisons between theoretical and experimental results are given in Ref. 2. The disagreement between the theoretical and experimental results under coswirl flow conditions may be due to the use of an isotropic diffusivity which does not include the effects of streamline curvature on turbulence. In this respect, it should be mentioned that algebraic closure models similar to that of Gibson[8] may yield satisfactory results. These models, however, are not yet ready for use in application-oriented studies. It should also be pointed out that the turbulence models used in this study were developed for well-known flows such as jets and boundary layers; their validity in arbitrary recirculating flows has never been demonstrated convincingly. In addition, the lack of accurate experimental measurements and inlet flow conditions, and the numerical errors associated with the use of upwind difference schemes are some other factors that contribute to the differences observed between the theoretical and experimental data.

References

[1] Ramos, J.I., "A Numerical Study of Incompressible, Turbulent, Confined, Swirling Flows. Part II: The Effect of the Inner Pipe Thickness," Report CO/80/5, Dept. of Mechanical Engineering, Carnegie-Mellon Univ., Pittsburgh, Pa., 1980.

[2] Ramos, J.I., "A Numerical Study of Turbulent Swirling Flows," Report CO/81/2, Dept. of Mechanical Engineering, Carnegie-Mellon Univ., Pittsburgh, Pa., 1981.

[3] Vu, B.T. and Gouldin, F.C., "Flow Measurements in a Model Swirl Flow," AIAA Paper No. 80-0076, Jan. 1980.

[4] Lilley, D.B., "Swirl Flows in Combustion: A Review," *AIAA Journal*, Vol. 15, Aug. 1977, pp. 1063-1078.

[5] Srinivasan, R. and Mongia, H.C., "Numerical Computations of Swirling Recirculating Flow: Final Report," NASA CR-165196, Sept. 1980.

[6]Abujelala, M.T. and Lilley, D.G., "Confined Swirling Flow Predictions," AIAA Paper No. 83-0316, Jan. 1983.
[7]Habib, M.A. and Whitelaw, J.H., "Velocity Characteristics of Confined Coaxial Jets with and without Swirl," *Journal of Fluids Engineering*, Vol. 102, March 1980, pp. 47-53.
[8]Gibson, M.M., "An Algebraic Stress and Heat-Flux Model for Turbulent Shear Flow with Streamline Curvature," *International Journal of Heat and Mass Transfer*, Vol. 21, Dec. 1978, pp. 1609-1617.

Effect of Thermal Gradient on Frequencies of a Wedge-Shaped Rotating Beam

J.S. Tomar* and Rita Jain†
University of Roorkee, Roorkee, India

Introduction

SUFFICIENT work is available on vibrations of rotating beams[1-5] but none of them have considered the thermal effect on frequencies of bending vibrations. It is well known[6] that in the presence of a constant thermal gradient the elastic coefficients of homogeneous materials become functions of the space variables. Fanconneau and Marangoni[7] have investigated the effect of the nonhomogeneity caused by a thermal gradient on the natural frequencies of simply supported plates of uniform thickness.

The analysis presented in this Note considers bending vibrations of a wedge-shaped beam that could represent a turbine blade of simple geometry. The beam is attached to a disk of radius r as indicated in Fig. 1; the disk rotates with angular velocity Ω. It is restricted to the analysis of pure bending. Furthermore, the beam is subjected to one-dimensional temperature distribution along the length. Because the beam is wedge shaped, the area of cross section varies linearly. Consequently, $I(x)$, $b(x)$, and $A(x)$ are functions of x.

Analysis and Equation of Motion

The governing differential equation of transverse motion of a rotating beam of variable cross section, according to Schilhansl,[1] is

$$\frac{\partial^2}{\partial x^2}\left[EI(x)\frac{\partial^2 V}{\partial x^2}\right]+A(x)\rho\frac{\partial^2 V}{\partial t^2}=\frac{\partial^2 M}{\partial x^2} \tag{1}$$

where, using $\delta=[1-A(L)/A(0)]$

$$A(x)=A(0)\left(1-\delta\frac{x}{L}\right)$$

$$I(x)=\frac{A(0)}{12}\left[b^2(0)\left(1-\delta\frac{x}{L}\right)^3+\left(1-\delta\frac{x}{L}\right)t_1^2\right]$$

and

$$\frac{\partial^2 M}{\partial x^2}=\rho A(0)\Omega^2\left[\left\langle r(L-x)+\left(1-\delta\frac{r}{L}\right)\frac{L^2-x^2}{2}-\delta\frac{(L^3-x^3)}{3L}\right\rangle\frac{\partial^2 V}{\partial x^2}-\left\langle r+\left(1-\delta\frac{r}{L}\right)x-\delta\frac{x^2}{L}\right\rangle\frac{\partial V}{\partial x}+\left(1-\delta\frac{x}{L}\right)\sin^2\Psi V\right]$$

Equation (1), when put in terms of dimensionless variable $\xi=x/L$, takes the form

$$D\frac{\partial^4 V}{\partial\xi^4}+2D_{,\xi}\frac{\partial^3 V}{\partial\xi^3}+D_{,\xi\xi}\frac{\partial^2 V}{\partial\xi^2}+L^4\rho A(0)(1-\delta\xi)\frac{\partial^2 V}{\partial t^2}=L^4\rho A(0)\Omega^2\left[\left\langle\frac{r}{L}(1-\xi)+\frac{(1-\xi^2)}{2}\left(1-\delta\frac{r}{L}\right)-\frac{\delta}{3}(1-\xi^3)\right\rangle\frac{\partial^2 V}{\partial\xi^2}-\left\langle\frac{r}{L}+\left(1-\delta\frac{r}{L}\right)\xi-\delta\xi^2\right\rangle\frac{\partial V}{\partial\xi}+(1-\delta\xi)\sin^2\Psi V\right] \tag{2}$$

where

$$D=\frac{EA(0)}{12}[b^2(0)(1-\delta\xi)^3+(1-\delta\xi)t_1^2] \tag{3}$$

The comma followed by a subscript denotes partial differentiation with respect to the variable.

It is assumed that the beam is subjected to a steady one-dimensional temperature distributed along the length, i.e., in the x direction

$$T=T_0(1-\xi) \tag{4}$$

where T denotes the temperature excess above the reference temperature at any point at a distance $\xi=x/L$ and T_0 denotes the temperature excess above the reference temperature at the end $x=L$ or $\xi=1$.

The temperature dependence of the modulus of elasticity for most of the engineering material is

$$E(T)=E_1(1-PT) \tag{5}$$

where E_1 is the value of the modulus of reference temperature, i.e., at $T=0$ along the x direction.

Taking the temperature at the end of the beam as the reference temperature, i.e., at $\xi=1$, the modulus variation becomes

$$E(\xi)=E_1[1-\alpha(1-\xi)] \tag{6}$$

where

$$\alpha=PT_0 \qquad (0\le\alpha\le 1)$$

Substitution of Eq. (6) in Eq. (3) gives

$$D=E_1[1-\alpha(1-\xi)]\left\{\frac{A(0)}{12}[b^2(0)(1-\delta\xi)^3+t_1^2(1-\delta\xi)]\right\} \tag{7}$$

Determination of the Frequency Parameter

The solution of Eq. (2) can be assumed to be of the form

$$V(\xi,t)=A_1 f(\xi)e^{i\omega t} \tag{8}$$

Received Jan. 13, 1983; revision received Aug. 3, 1983.

*Professor, Department of Mathematics.
†Research Fellow, Department of Mathematics.